TOWARDS FRAGILITY ANALYSIS FOR CONCRETE BUILDINGS IN FIRE: RESIDUAL CAPACITY OF CONCRETE COLUMNS

8th International Conference on Structures in Fire
Shanghai, China, June 11-13, 2014

TOWARDS FRAGILITY ANALYSIS FOR CONCRETE BUILDINGS IN FIRE: RESIDUAL CAPACITY OF CONCRETE COLUMNS

David Rush*, Luke Bisby*, Ioanna Ioannou and Tiziana Rossetto ****

* BRE centre for Fire Safety Engineering, School of Engineering, University of Edinburgh, UK
e-mails: d.rush@ed.ac.uk, l.bisby@ed.ac.uk

** EPICentre, University College London, UK
e-mail: ioanna.ioannou@ucl.ac.uk, t.rossetto@ucl.ac.uk

Keywords: Fragility analysis, Reinforced concrete, Residual strength, Probabilistic design.

Abstract. *Fire engineering a building, in general, has one central performance objective – life safety – and property protection is rarely explicitly considered. The engineering is typically based on only one possible fire, which may not represent the most onerous scenario (or may be much too onerous to be considered realistic). Taking inspiration from fragility analyses used in seismic engineering, this paper explores the relationship between post-fire structural response and the 'intensity' of the fire. The influence of 27 different parametric fires on the residual capacity of a reinforced concrete column is theoretically assessed and it is shown that the ventilation factor used to define the fire curves has a clear influence on the calculated residual response of the column, both in terms of peak fire temperature but also total duration of fire exposure. This paper represents a first step towards developing quantified fragility analyses for probabilistic structural fire design of concrete buildings.*

1 INTRODUCTION

The 2011 earthquake in Christchurch, NZ, caused a great deal of damage to the city, which is expensive to repair or replace. The high level of damage and the cost of reinstatement was shocking to the public and insurers alike, however from an engineering perspective the vast majority of buildings performed "very well" on the basis of the explicit design objectives used to engineer them [1]. This suggests that society is largely unaware of the true "performance" objectives that are used by structural engineers in design, whether for earthquake or fire engineering; it may be that a higher 'level' of property protection is actually expected by society (however this is rarely noticed due to the infrequency of severe earthquales – or fires). In current fire engineering design there is, in general, no accept means of quantifying property protection goals (or of rationally accounting for these goals in design), and design is instead based almost entirely on life safety and property protection is rarely explicitly considered – there is typically little or no consideration of 'damage,' rather simply a pass/fail assessment usually consisting of prescribed fire resistance criteria and times. Furthermore this assessment is usually based on a standard fire (e.g. ISO-834 [2]) that represents only one, physically impossible, fire, and may not represent the most onerous (or more realistic) fire insult that a structure might experience [3]. Real fires are more akin to earthquakes from a risk perspective, no two are the same, and a single fire in any given building will affect different elements within the structure differently. How to assess and quantify the damage caused by a real fire in a real building, so that reuse/repair/replace plans can be developed, is an open question.

The seismic community have, for many years, applied concepts of 'fragility analysis,' where the probability of a structural system reaching a given *damage state* is assessed as a function of some measure of *intensity* (e.g. peak ground acceleration used in earthquake engineering). From this assessment, designers and insurers can calculate the *expected costs* of repair or replacement of the building. Therefore a *fragility analysis* allows designers to rationally and quantifiably account for the

risks and *costs* associated with the *range* of possible earthquakes, and explicitly accounts for property protection as a desirable design goal. This paper is a step towards quantifying fragility analyses and the critical parameters for probabilistic performance-based fire design of concrete structures..

2 FRAGILITY ANALYSES

Fragility analysis thinking has started to appear in the structural fire engineering literature (e.g. [4]), largely for steel-frames structures, however fragility concepts have specific relevance for concrete structures since concrete structures may perform better: (a) in real rather than standard fires; and (b) than other types of construction in terms of property protection considerations (provided that heat-induced concrete cover spalling is avoided).

Equation 1 represents the probabilistic risk assessment of a building affected by a hazard for a given period of time; for example fires/year. The risk is defined as consequence × hazard, where the consequence is estimated by three stochastic relationships; intensity measure (*IM*) to response measure (*RM*); RM to damage measure (*DM*); and DM to loss or some other decision variable (*DV*). In other words, given the likelihood of an event occurring in a building, the *IM* forces the building to have a response, *RM*, which leads to a measure of damage, *DM*, and subsequent level of loss, *DV*. The fundamental aim of the reasoning represented by Eq. 1 is to provide quantified annual expected loss metrics for a given structure based on the magnitude and risk of a hazard occurring. A fragility analysis is a component of the risk assessment, and consists of two analyses: (1) structural and (2) damage analysis, thus linking the probability of different damage (*DM*) occurring for a given fire intensity (*IM*).

$$gDV = \iiint \underbrace{P[DV|DM]}_{\text{Loss analysis}} \underbrace{dP[DM|RM]}_{\text{Damage analysis}} \underbrace{dP[RM|IM]}_{\text{Structural analysis}} \underbrace{dg_{IM}}_{\text{Hazard analysis}} \tag{1}$$

The advantage of Eq. 1 is that it implicitly assumes that that each of the four analyses can be conducted independently, and that the final products of the conditional distributions presented in Eq. 1 can be coupled to estimate the risk to the building over a specified period of time.

The determination of suitable intensity measures is not straightforward since *IM*s also depend on the effect that a hazard has on the structure and the *RM* being assessed (i.e. if deflections were the *RM* then peak rebar temperatures might be the *IM*, however if structural capacity is the *RM* then the area under the fire curve might be a more appropriate *IM*). Ideally a large database of experimental and real fire structural response data would inform decisions on which *IM*s and *RM*s are most suitable for use in designing concrete buildings; however, there is a paucity of data, and thus computational analysis and expert opinion must be relied upon. Once the *IMs* and *RMs* have been decided, *DM*s can be determined (as has previously been attempted in [5]), along with the costs associated with the *DM*s, through expert opinion. The risk assessment framework of Eq. 1 estimates the risk to buildings affected by all possible fires likely to occur in a given interval and allows designers to design specifically for property protection.

3 EXAMPLE: AXIALLY LOADED REINFORCED CONCRETE COLUMN

In this paper the relationship between *IM* and *RM* for an example reinforced concrete column is assessed through computational analysis, rather than experimentally, given that there are a range of possible design fires that could affect a concrete column (see Table 1). The *RM* being assessed in the current analysis is the residual axial load capacity (strength) of the concrete column. This depends on the maximum temperature experienced within the cross-section, since temperature adversely influences the residual stress-strain relationships of both reinforcing steel and concrete. The maximum temperatures

within the cross-section were calculated (by finite elements) at several depths and under several different time-temperature histories that each represents one possible *IM*.

Table 1: Details of concrete column used in the current study.

L (m)	Size (mm)	K	$l_{e,re}$ (KL - m)	Bars no. × size	A_s/A_c	Cover (mm)	f'_c/f_{cu} (MPa)	f_y (MPa)	E_s (MPa)
3	300 × 300	0.7	2.1	8 × 20 mm Ø	2.8%	30	35/45	500	205000

3.1 Parametric fire calculations

The initial stage of the analysis was to parameterise the design space in terms of *IM*, so a family of 27 design fires have been created based on the Eurocode parametric fires [2]. The fires are initially defined by varying three parameters (A: compartment size, B: fuel load, and C: ventilation), each with three values (1, 2, and 3) to give the broad range of 27 fire intensities outlined in Table 2. Each design fire has two parts; a growth phase and a cooling phase. The growth phase of the temperature (Θ_g) is defined by:

$$\Theta_g = 20+1325\cdot\left(1-0.324e^{-0.2t^*}-0.204e^{-1.7t^*}-0.472e^{-19t^*}\right) \quad (2)$$

where $t^* = t\cdot\Gamma$, where t is the time in hours, and the dimensionless ratio $\Gamma = (O/b)^2/(0.04/1160)^2$, O is the opening factor (limited to a maximum of 0.2 and minimum of 0.02).

The growth rate of the fire determines the maximum temperature that Eq. 2 can reach and is limited by the greater of t_{lim} (Table 2) or $t_{max} = (0.2\text{x}10^{-3}\cdot q_{t,d})/O$. If $t_{lim} > t_{max}$ the fire is deemed fuel controlled; if $t_{lim} < t_{max}$ the fire is deemed ventilation controlled. The design fire load density, $q_{t,d}$, is a function of the fuel load, $q_{f,k}$, which takes into account the risk of fire activation and firefighting measures in relation to the floor and total surface areas of the compartment (Annex E of [2]). The cooling phase of the design fire is linear and is dependent on the size of t_{max} with larger values having shallower gradients.

Table 2: Parametric curve calculation input parameters [2].

	Variables				Constants	
	Room size[a] A_f (m^2)		Fuel load[b] $q_{f,k}$ (kg/m^2)	Opening factor O (m$^{1/2}$)	Boundary Enclosure $b = \sqrt{(\rho.\lambda.c)}$	Enclosure height: *3m*
	A		B	C		
1	9	3 × 3	612[c]	0.02	ρ = 2300 kg/m^3	Growth rate*:*
2	250	15.8 × 15.8	780[d]	0.066149[f]	λ = 1.6 W/mK,	*Medium*
3	500	22.4 × 22.4	948[e]	0.2	c = 1000 J/kgK	t_{lim} = 20 mins

[a] Maximum of 500m^2, [b] Dwelling fuel loads, [c] value B1 = B2 - (B3 - B2), [d] average, [e] 80%ile, [f] opening factor required for $\Gamma = 1$; approximation of standard time temperature curves.

Table 3 presents the maximum temperatures obtained from Eq. 2 for the 27 parametric fires, whilst Figure 1 shows the 27 design fire time-temperature curves based on the Eurocode's parametric fires [2]. The black marker curves are all ventilation controlled fires; white marker curves are approximations of the standard time-temperature curves and are ventilation controlled; and the grey marker curves are in general fuel load controlled, thus many have the same profile.

3.2 Thermal modelling of cross-section and structural analysis of RC column

A three stage process is required to calculate the residual capacity of the RC column under the 27 different fires shown in Figure 1: Stage (1) is to conduct a heat transfer analysis within the cross section for the entire length of fire duration; Stage (2) is to discretize the cross-section into elements in which the temperature is assumed to be uniform; and Stage (3) is to calculate the structural capacity of the column using maximum temperature dependent residual constitutive material relationships.

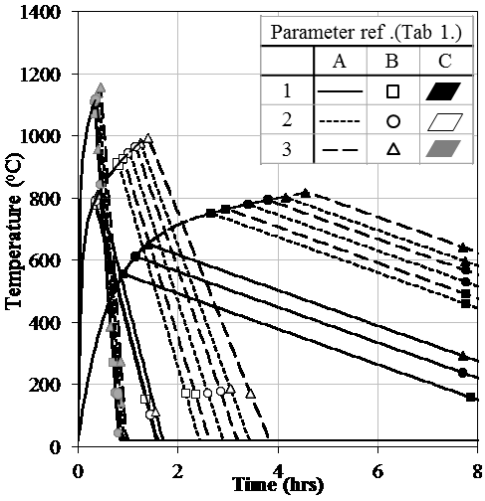

Figure 1: Twenty-seven parametric fire curves.

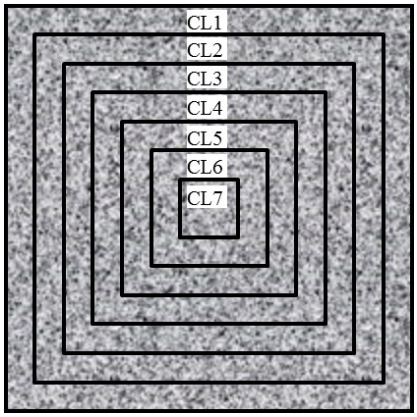

Figure 2: Square segmentation (CL*i* = concrete layer *i*).

Table 3: Maximum fire temperatures and averaged maximum layer temperatures.

Fire	Maximum temperatures - θmax (°C)								Capacity	
A-B-C (Table 2)	Fire (Θ_g)	CL1	CL2	CL3	CL4	CL5	CL6	CL7	$N_{re,fi}$ (kN)	RSI^a
000	N/A	20 – Ambient							4255	1.00
1-1-1	556	405	363	344	335	332	331	331	3447	0.81
1-1-2	789	489	337	258	218	206	204	203	3518	0.83
1-1-3, 1-2-3, 1-3-3, 2-1-3, 3-1-3	1110	779	460	313	247	230	227	226	2962	0.70
1-2-1	613	473	425	403	394	390	389	389	3158	0.74
1-2-2	793	497	344	263	222	210	207	207	3493	0.82
1-3-1	653	523	472	448	439	435	434	433	2873	0.68
1-3-2	818	543	379	292	247	232	229	229	3350	0.79
2-1-1	751	667	610	584	573	569	567	567	1943	0.46
2-1-2	911	716	534	428	370	347	342	341	2629	0.62
2-2-1	780	715	661	635	624	619	618	618	1701	0.40
2-2-2	948	781	604	495	435	411	404	403	2276	0.53
2-2-3	1113	784	465	316	249	232	229	228	2947	0.69
2-3-1	804	752	704	679	667	663	662	661	1513	0.36
2-3-2	978	833	664	556	497	472	466	464	1965	0.46
2-3-3	1143	838	519	356	280	258	255	254	2760	0.65
3-1-1	765	690	634	608	597	593	591	591	1838	0.43
3-1-2	928	748	568	459	400	376	370	369	2464	0.58
3-2-1	794	737	687	661	650	645	644	644	1654	0.39
3-2-2	965	813	640	531	471	447	440	439	2264	0.53
3-2-3	1130	814	496	339	267	247	244	243	3157	0.74
3-3-1	818	775	731	706	695	691	689	689	1461	0.34
3-3-2	995	863	701	596	538	514	507	506	1889	0.44
3-3-3	1160	874	554	384	301	277	273	272	2921	0.69

[a] RSI = residual strength index = $N_{re,fi}/N_{re,fi(000)}$

3.2.1 Thermal analysis

The 27 design fires were applied to a theoretical 300 × 300 mm RC column cross-sections and a finite element method (FEM) heat transfer analysis conducted (using ABAQUS). The density, thermal conductivity, and specific heat capacity of concrete were assumed to be constant with values of ρ = 2300 kg/m^3, λ = 1.6 W/mK, and c = 1000 J/kgK (no water), respectively. The model also employed the net heat flux method of heat transfer as suggested by Eurocode 1 [2] with the resultant emissivity of concrete and fire is 0.7 and the convective heat flux coefficient of 25 W/m^{2}K

3.2.2 Cross-section discretization and layer temperatures

Once the FEM analysis had been completed, the cross-section was discretized into ringed segments of equal thickness in which the temperature is assumed to be uniform. Square sections experience higher temperatures at the corners than at the middle of the flat faces which suggests that a fully discretized 2D analysis is required, however precedence exists [6] to assume an equivalent uniform temperature in each concrete layer in the square section, provided that the uniform temperature chosen for the layer leads to the same (or smaller) contribution to either the plastic resistance in compression or the cross-section's flexural stiffness as would a more complete summation of a 2D grid of concrete elements. This means that a full 2D discretization was not required in this analysis and each of the concrete rings is assumed to have a uniform maximum temperature, averaged from the elemental temperatures in that layer.

The square section was discretised into seven concrete layers,as shown schematically in Figure 2. Clearly, the more layers that are taken the more refined the prediction, however seven layers were used in a previous study conducted [6] by the authors on concrete filled steel hollow sections and was found to predict temperatures and response adequately. The maximum temperatures experienced in each layer are presented in Table 3. It was assumed that the temperature in the rebar was the same temperature as the concrete layer in which is resides (i.e. CL2).

3.2.3 Structural analysis

The calculation of residual capacity of the RC column follows the similar method to Eurocode 4 Annex H [7]. Using a simple spreadsheet analysis the residual capacity of the column, $N_{re,fi}$, is determined from the design axial buckling load of the column during fire. This is found by assuming that all materials experience the same strain at a given time and temperature and then calculating the strain at which the elastic critical or Euler buckling load, $N_{re,cr}$, is equal to the plastic (crushing) resistance to compression of the cross section, $N_{re,pl,Rd}$:

$$N_{re,fi} = N_{re,cr} = N_{re,pl,Rd} \tag{3}$$

$N_{re,cr}$ (Eq. 4) is the summation of the elastic flexural rigidities of the concrete layers (subscript c), and internal steel reinforcement (subscript s), whilst $N_{re,pl,Rd}$ (Eq. 5) is the summation of the crushing strength contributions of the respective materials and layers:

$$N_{re,cr} = \pi^2 \left[\sum E_{c,\theta\max,\sigma} I_c + E_{s,\theta\max,\sigma} I_s \right] / l_{e,re}^2 \tag{4}$$

$$N_{re,pl,rd} = \sum A_c \sigma_{c,\theta\max} + A_s \sigma_{s,\theta\max} \tag{5}$$

In the above equations, $E_{i,\theta max,\sigma}$ is the tangent modulus of the stress-strain relationship for the material i at maximum temperature θmax and for a stress $\sigma_{i,\theta max}$, I_i is the second moment of area the material i, A_i is the cross-sectional area of material i, and $l_{e,re}$ is the residual buckling length of the column, which in this analysis is assumed to be the same as in the fire situation.

A bi-linear residual stress-strain materials model is assumed for steel [8], as shown in Figure 3(a), and given by:

$$\sigma_a = \begin{cases} E_a\left(\theta_{a,\max}\right)\cdot\varepsilon_a & \varepsilon_a \le \varepsilon_{sy}(T) \\ f_{sy}\left(\theta_{a,\max}\right) + E_1\left(\theta_{a,\max}\right)\cdot\left[\varepsilon - \varepsilon_{sy}\left(\theta_{a,\max}\right)\right] & \varepsilon_a > \varepsilon_{sy}(T) \end{cases} \quad (6)$$

where $E_a(\theta_{a,max})$ is the Young's modulus of steel; $\varepsilon_{sy}(\theta_{a,max}) = f_{sy}(\theta_{a,max})/E_a(\theta_{a,max})$; $E_1(\theta_{a,max}) = 0.01 \cdot E_a(\theta_{a,max})$; and $f_{sy}(\theta_{a,max})$ is the yield strength of the steel after exposure to high temperature ($\theta_{a,max}$). This last term can be expressed as [8]:

$$f_{sy}\left(\theta_{a,\max}\right) = \begin{cases} f_{sy} & \theta_{a,\max} \le 400^o C \\ f_{sy} \cdot \left[1 + 2.33\times10^{-4}\cdot\left(\theta_{a,\max} - 20\right) - 5.88\times10^{-7} \cdot\left(\theta_{a,\max} - 20\right)^2\right] & \theta_{a,\max} > 400^o C \end{cases} \quad (7)$$

Residual stress-strain materials models for confined concrete are also proposed in [8] and [9], and are used in this analysis but with the confinement factor set to zero. The resulting stress-strain relationship is given in Eq. 8 of Table 4 and shown graphically in Figure 3 (b).

Table 4: Residual strength design equations from [8], [9] with confinement factor set to zero.

$$y = \begin{cases} x & x \le 1 \\ \dfrac{x}{\left(0.75\cdot f_{ck}^{0.1}\right)\cdot(x-1)^{\eta} + x} & x > 1 \end{cases} \quad (8)$$

where: $y = \sigma/\sigma_{0p}\left(\theta_{c,\max}\right)$ $x = \varepsilon/\varepsilon_{0p}\left(\theta_{c,\max}\right)$	$\sigma_{0p}\left(\theta_{c,\max}\right) = f_{cp}\left(\theta_{c,\max}\right)$
$\varepsilon_{0p}\left(\theta_{c,\max}\right) = \varepsilon_{ccp}\left(\theta_{c,\max}\right) + \left[1330 + 760\cdot\left(\dfrac{f_c'}{24} - 1\right)\right]$	$\eta = 1.6 + 1.5\cdot\left(\dfrac{\varepsilon_{0p}\left(\theta_{c,\max}\right)}{\varepsilon}\right)$
$\varepsilon_{ccp}\left(\theta_{c,\max}\right) = \left[1 + \left(1500\cdot\theta_{c,\max} + 5\cdot{\theta_{c,\max}}^2\right)\times10^{-6}\right] \cdot\left(1300 + 12.5\cdot f_c'\right)$	$f_{cp}\left(\theta_{c,\max}\right) = \dfrac{f_c'}{1 + 2.4\cdot\left(\theta_{c,\max} - 20\right)^6\times10^{-17}}$

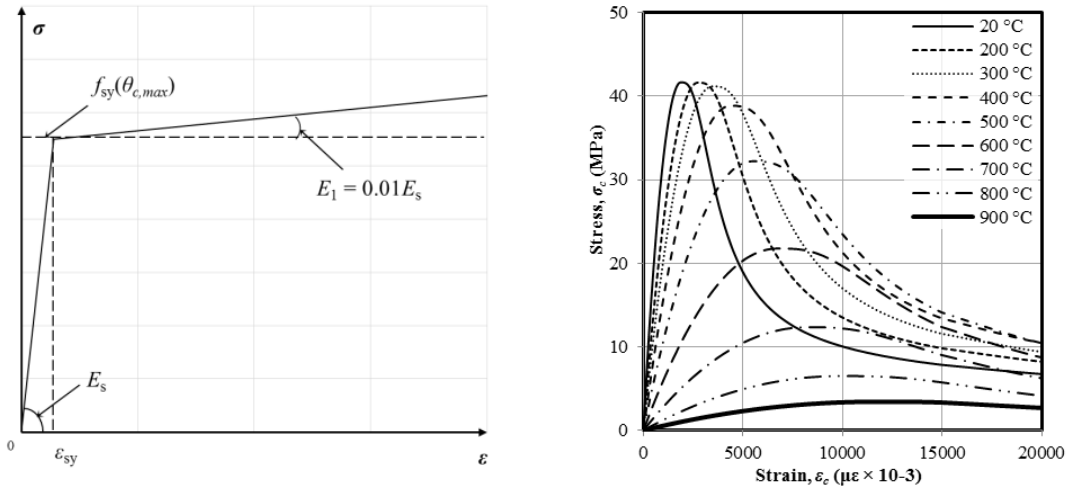

Figure 3: Residual mechanical stress-strain relationships for (a) steel (assumed bi-linear) and (b) unconfined concrete at different maximum temperatures.

4 RESULTS AND ANALYSIS OF CALCULATIONS

Table 3 shows the residual capacities of the column, calculated using Eq.3, after exposure to each of the 27 different time-temperature fire curves, and also shows the relative residual strength (RSI = $N_{re,fi}/N_{re,fi(000)}$) due to each thermal exposure.

4.1 General response

The residual strength index's range from 0.34 to 0.83 depending on the fires involved. It should be noted that in the calculation of the structural capacity, the strain level that produced the maximum capacity was equal to yield strain of the steel, ε_{sy}. This is because, in the material models used, strain levels greater than this value the flexural stiffness of the rebar reduces to 1% of E_a, thus reducing the columns buckling capacity below the crushing capacity of the column. The stress-strain relationship for steel is obviously a simplified model and does not necessarily reflect what would occur in real life.

Table 3 also shows the RSI in general reduces as either floor size and/or fuel load increases, for instance fire 2-1-1 and 3-1-1 produce RSIs of 0.46 and 0.43, respectively. This trend cannot be said for the influence of the opening factor, where the "standard" fire approximation produces the largest RSI when all other factors are equal, for instance fires 1-1-1, 1-1-2, 1-1-3 produce RSIs of 0.81, 0.83, 0.70 respectively. The authors believe that this is again due to the unrealistic and simplified bi-linear steel stress strain relationship. The columns maximum capacity in this analysis is dependent on ε_{sy}, which in turn is dependent on the temperature experienced in the steel. The higher the temperatures are the larger the yield strain, ε_{sy}, and thus, in these models, larger strains are able to develop in the cross-section and in particular the concrete. When the temperatures in the concrete are relatively low (<400°C), but the temperature experienced in the rebar (CL2) are comparatively high (>400°C), then the concrete benefits from the increase in ε_{sy} and the column can take more load. Therefore, in this modelling analysis, columns exposed to a slightly more intense fire can actually have more residual strength.

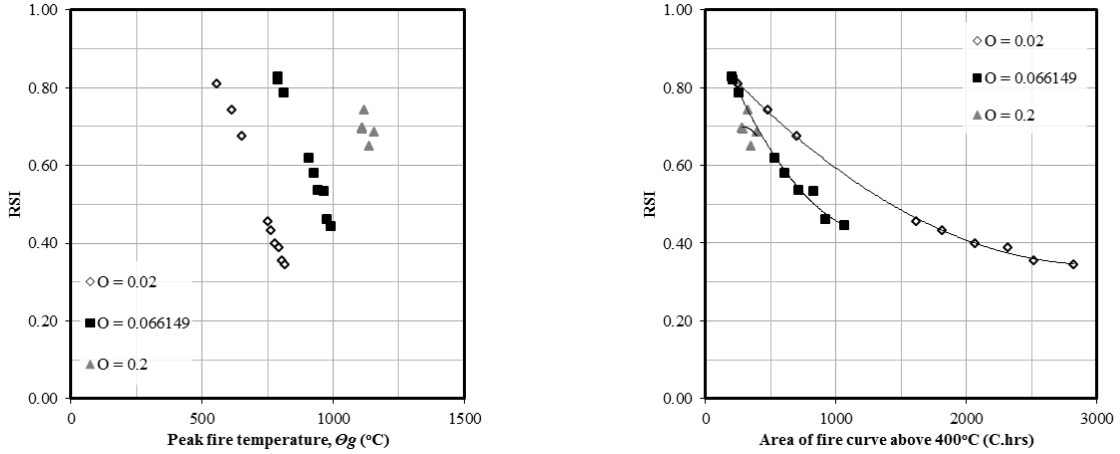

Figure 4: Residual strength index (RSI) relationships to (a) peak fire temperature and (b) area of the fire curve above 400°C; data in both figures separated by opening factor, *O*.

4.2 Relationship of response measure (*RM*) to intensity measure (*IM*)

As mentioned previously, fragility analyses require the appropriate selection of intensity measure (*IM*). For unprotected steel this is relatively easy as steel has high thermal conductivity so the response is highly dependent on the temperature of the fire. Concrete, however, has comparatively low thermal conductivity so peak fire temperature as an intensity measure (*IM*) cannot necessarily capture the full response of the concrete column. This is shown in Figure 4(a) that compares the peak fire temperature to the RSI where, for approximately the same peak fire temperature, the RSI can differ by over 100%. Figure 4(a) shows that the response is influenced by the opening factor, *O*. The opening factor influences both the peak fire temperature and the length of time the fire burns for. Small opening factors will

produce longer cooler fires, compared to larger opening factors that will produce shorter hotter fires (see Figure 1). Figure 4(a) shows that the longer, lower temperature fires (small *O*), have a greater effect on the residual strength of the concrete column, thus the time of fire exposure to the concrete is important.

Figure 4(b) compares the RSI to the area under the fire curve for gas temperatures above 400°C, where the "area of the fire curve above 400°C" represents a measure of the amount of energy that the concrete column is exposed to above the threshold of 400°C (the threshold of 400°C was chosen due to the noticeable change in response of the concrete column occurs at temperatures in excess of 400°C as a result of the stress-strain models used in this analysis). Figure 4(b) again shows obvious trends in relation to the influence of the opening factor on the RSI, but also shows that the response is not solely due to the amount of energy absorbed by the concrete column. Figure 4 shows that there is an interaction between the ventilation, "area" of the fire, and temperature that needs further investigation to fully understand.

5 CONCLUSION AND RECCOMENDATIONS

The aim of this paper was to initiate the theoretical analysis and critical thinking required to promote the use of probabilistic design methodologies within structural fire engineering of concrete structures. Therefore this paper presented a brief summary of a popular framework that is being employed within the probabilistic design in earthquake engineering and is being developed for use in structural fire engineering. The paper then presented an initial analysis of the residual strength capacity of a reinforced concrete column exposed to twenty-seven different possible fires. The analysis showed that the residual strength capacity response measure of the column is dependent on more complex measures of fire intensity than just peak fire temperature, but is also influenced by the length of time the column is exposed to the thermal insult; short hot fires produce less damage compared to longer shallower fires.

More work is required not only to understand the appropriate intensity measures to use for the post-fire residual strength of concrete columns, but also for developing appropriately verified residual strength material models for both steel and concrete. This paper has presented a first step towards understanding fragility analyses and intensity measures for probabilistic design of concrete structures in fire.

REFERENCES

[1] W. Kam, S. Pampanin, and K. Elwood, "Seismic performance of reinforced concrete buildings in the 22 Feburary Christchurch (Lyttelton) eathquake," *Bull. NZ Soc. Earthq. Eng.*, vol. 44, 2011.

[2] CEN, "BS EN 1991-1-2: Eurocode 1: Actions on structures; Part 1-2: General Actions - Actions on structures exposed to fire," Brussels, Belgium, 2009.

[3] J. Gales, C. Maluk, and L. Bisby, "Large-scale structural fire testing - how did we get here, where are we, and where are we going?," in *ICEM 15 - Porto*, 2012, pp. 1–22.

[4] S. Devaney, D. Lange, A. Usmani, and C. Manohar, "Adapting the peer methodology to account for the fire hazard," in *PLSE*, 2012.

[5] The Concrete Society, *Assessment, design and repair of fire-damaged concrete structures - Technical report no. 68*. Camberley UK: The Concrete Society, 2008.

[6] D. Rush, L. Bisby, B. Lane, and A. Melandinos, "Structural performance of unprotected concrete-filled steel hollow sections in fire: A review and meta-analysis of available test data," *Steel Compos. Struct.*, vol. 12, no. 4, pp. 325–352, 2012.

[7] CEN, "BS EN 1994-1-2: Eurocode 4: Design of composite steel and concrete structures; Part 1-2: Structural Fire Design," Brussels, Belgium, 2005.

[8] L. H. Han and J. S. Huo, "Concrete filled hollow structural steel columns after exposure to ISO-834 standard fire," *J. Struct. Eng.*, vol. 129, no. 1, p. 68, 2003.

[9] H. Yang, L. H. Han, and Y. C. Wang, "Effects of heating and loading histories on post-fire cooling behaviour of concrete-filled steel tubular columns," *J. Constr. Steel Res.*, vol. 64, May 2008.